with HRP substrate kit (BIO-RAD). Results are expressed as absorbance at 405 nm of serum diluted 1:300.

RNA preparation, reverse transcription and PCR. RNA was extracted using TRIzol (GIBCO BRL) and reverse transcribed in 20 μl with Superscript II (GIBCO BRL). RT-PCR reactions were performed with serial dilutions of cDNA template using AmpliTaq Gold (Perkin Elmer). The following PCR conditions and primers were used: Igβ, 30 s at 94 °C, 60 s at 60 °C, 45 s at 72 °C for 30 cycles, 5′-CCATGGCCACACTGGTGCTGTC-3′ and 5′-CCTGAGT GGTTTGTGTAGCAGTG-3′; RAG1, 30 s at 94 °C, 60 s at 62 °C, 45 s at 72 °C, for 32 cycles, 5-CAACCAAGCTGCAGACATTCTAGCACTC-3′ and 5′-CAC GTCGATCCGGAAAATCCTGGCAATG-3′; endogenous RAG2, 30 s at 94 °C, 60 s at 60 °C, 45 s at 72 °C for 36 cycles, 5′-CACATCCACAAGCAGGAAGT ACAC-3′ and 5′-GGTTCAGGGACATCTCCTACTAAG-3′; β-actin, 30 s at 94 °C, 60 s at 62 °C, 45 s at 72 C for 25 cycles, 5′-TACCACTGGCATCGTG ATGGACT-3′ and 5′-TTTCTGCATCCTGTCGGCAAT. To detect RSS breaks, DNA preparation in agarose plugs, linker ligation, PCR and Southern blot hybridization were performed as described[30]. Igβ PCR was performed using the following conditions and primers: 30 s at 94 °C, 30 s at 60 °C, 80 s at 72 °C for 32 cycles, 5′-TCACTGCTACACAAACCACTCAGG-3′ and 5′-AGTTCCGTGC-CACAGCTGTCGG-3′. The Igβ amplification product was visualized using ethidium bromide.

1. Gay, D., Saunders, T., Camper, S. & Weigert, M. Receptor editing: an approach by autoreactive B cells to escape tolerance. *J. Exp. Med.* **177,** 999–1008 (1993).
2. Tiegs, S. L., Russell, D. M. & Nemazee, D. Receptor editing in self-reactive bone marrow B cells. *J. Exp. Med.* **177,** 1009–1020 (1993).
3. Grawunder, U. *et al.* Down-regulation of RAG1 and RAG2 gene expression in preB cells after functional immunoglobulin heavy chain rearrangement. *Immunity* **3,** 601–608 (1995).
4. Yang, X. W., Model, P. & Heintz, N. Homologous recombination based modification in *Escherichia coli* and germline transmission in transgenic mice of a bacterial artificial chromosome. *Nature Biotechnol.* **15,** 859–865 (1997).
5. Lin, W. C. & Desiderio, S. Regulation of V(D)J recombination activator protein RAG-2 by phosphorylation. *Science* **260,** 953–959 (1993).
6. Allman, D. M., Ferguson, S. E. & Canero, M. P. Peripheral B cell maturation. I. Immature peripheral B cells in adults are heat-stable antigenhi and exhibit unique signaling characteristics. *J. Immunol.* **149,** 2533–2540 (1992).
7. Rolink, A. G., Andersson, J. & Melchers, F. Characterization of immature B cells by a novel monoclonal antibody, by turnover and by mitogen reactivity. *Eur. J. Immunol.* **28,** 3738–3748 (1998).
8. Han, S., Zheng, B., Schatz, D. G., Spanopoulou, E. & Kelsoe, G. Neoteny in lymphocytes: Rag1 and Rag2 expression in germinal center B cells. *Science* **274,** 2094–7 (1996).
9. Hikida, M. *et al.* Reexpression of RAG-1 and RAG-2 genes in activated mature mouse B cells. *Science* **274,** 2092–2094 (1996).
10. Hertz, M., Kouskoff, V., Nakamura, T. & Nemazee, D. V(D)J recombinase induction in splenic B lymphocytes is inhibited by antigen-receptor signalling. *Nature* **394,** 292–295 (1998).
11. Meffre, E. *et al.* Antigen receptor engagement turns off the V(D)J recombination machinery in human tonsil B cells. *J. Exp. Med.* **188,** 765–772 (1998).
12. Forster, I. & Rajewsky, K. The bulk of the peripheral B-cell pool in mice is stable and not rapidly renewed from the bone marrow. *Proc. Natl Acad. Sci. USA* **87,** 4781–4784 (1990).
13. Papavasiliou, F. *et al.* V(D)J recombination in mature B cells a new mechanism for diversification of antibody responses. *Science* **278,** 298–301 (1997).
14. Russell, D. M. *et al.* Peripheral deletion of self-reactive B cells. *Nature* **354,** 308–311 (1991).
15. Hartley, S. B. *et al.* Elimination from peripheral lymphoid tissues of self-reactive B lymphocytes recognizing membrane-bound antigens. *Nature* **353,** 765–769 (1991).
16. Pelanda, R. *et al.* Receptor editing in a transgenic mouse model: site, efficiency, and role in B cell tolerance and antibody diversification. *Immunity* **7,** 765–775 (1997).
17. Han, S. *et al.* V(D)J recombinase activity in a subset of germinal center B lymphocytes. *Science* **278,** 301–305 (1997).
18. von Boehmer, H. & Fehling, H. J. Structure and function of the pre-T cell receptor. *Annu. Rev. Immunol.* **15,** 433–452 (1997).
19. Turka, L. A. *et al.* Thymocyte expression of RAG-1 and RAG-2; termination by T cell receptor cross-linking. *Science* **253,** 778–781 (1991).
20. Colclough, C., Perry, R. P., Karjalainen, K. & Weigert, M. Aberrant rearrangements contribute significantly to the allelic exclusion of immunoglobulin gene expression. *Nature* **290,** 372–378 (1981).
21. Storb, U. in *Immunoglobulin Genes* (eds Honjo, T. & Alt, F.) 345–363 (Academic, San Diego, 1995).
22. Melamed, D., Benschop, R. J., Cambier, J. C. & Nemazee, D. Developmental regulation of B lymphocyte immune tolerance compartmentalizes clonal selection from receptor selection. *Cell* **92,** 173–182 (1998).
23. Hartley, S. B. *et al.* Elimination of self-reactive B lymphocytes proceeds in two stages: arrested development and cell death. *Cell* **72,** 325–335 (1993).
24. Chen, C. *et al.* The site and stage of anti-DNA B-cell deletion. *Nature* **373,** 252–255 (1995).
25. Nussenzweig, M. C. *et al.* A human immunoglobulin gene reduces the incidence of lymphomas in c-Myc-bearing transgenic mice. *Nature* **336,** 446–460 (1988).
26. Costa, T. E., Suh, H. & Nussenzweig, M. C. Chromosomal position of rearranging gene segments influences allelic exclusion in transgenic mice. *Proc. Natl Acad. Sci. USA* **89,** 2205–2208 (1992).
27. Kitamura, D., Roes, J., Kuhn, R. & Rajewsky, K. A B-cell deficient mouse by targeted disruption of the membrane exons of the immunoglobulin μ-chain gene. *Nature* **350,** 423–426 (1991).
28. Schatz, D. G., Oettinger, M. A. & Baltimore, D. The V(D)J recombination activating gene, RAG-1. *Cell* **59,** 1035–1048 (1989).
29. Oettinger, M. A., Schatz, D. G., Gorka, C. & Baltimore, D. RAG-1 and RAG-2, adjacent genes that synergistically activate V(D)J recombination. *Science* **248,** 1517–1523 (1990).
30. Schlissel, M., Constantinesc, U. A., Morrow, T., Baxter, M. & Peng, A. Double-strand signal sequence breaks in V(D)J recombination are blunt, 5′-phosphorylated, RAG-dependent, and cell cycle regulated. *Genes Dev.* **7,** 2520–2532 (1993).

A SMAD ubiquitin ligase targets the BMP pathway and affects embryonic pattern formation

Haitao Zhu*†, **Peter Kavsak**†‡§∥, **Shirin Abdollah**‡∥, **Jeffrey L. Wrana**‡§∥ & **Gerald H. Thomsen***

**Department of Biochemistry and Cell Biology and Institute for Cell and Developmental Biology, State University of New York, Stony Brook, New York 11794-5215, USA*
‡ *Program in Developmental Biology, The Hospital for Sick Children, and* §*Department of Medical Genetics and Microbiology, University of Toronto, Toronto, Canada M5G 1X8*
† *These authors contributed equally to this work.*

....

The TGF-β superfamily of proteins regulates many different biological processes, including cell growth, differentiation and embryonic pattern formation[1–3]. TGF-β-like factors signal across cell membranes through complexes of transmembrane receptors known as type I and type II serine/threonine-kinase receptors, which in turn activate the SMAD signalling pathway[4,5]. On the inside of the cell membrane, a receptor-regulated class of SMADs are phosphorylated by the type-I-receptor kinase. In this way, receptors for different factors are able to pass on specific signals along the pathway: for example, receptors for bone morphogenetic protein (BMP) target SMADs 1, 5 and 8, whereas receptors for activin and TGF-β target SMADs 2 and 3. Phosphorylation of receptor-regulated SMADs induces their association with Smad4, the 'common-partner' SMAD, and stimulates accumulation of this complex in the nucleus, where it regulates transcriptional responses. Here we describe Smurf1, a new member of the Hect family of E3 ubiquitin ligases. Smurf1 selectively interacts with receptor-regulated SMADs specific for the BMP pathway in order to trigger their ubiquitination and degradation, and hence their inactivation. In the amphibian *Xenopus laevis*, *Smurf1* messenger RNA is localized to the animal pole of the egg; in *Xenopus* embryos, ectopic Smurf1 inhibits the transmission of BMP signals and thereby affects pattern formation. Smurf1 also enhances cellular responsiveness to the Smad2 (activin/TGF-β) pathway. Thus, targeted ubiquitination of SMADs may serve to control both embryonic development and a wide variety of cellular responses to TGF-β signals.

To identify new components of the SMAD pathway, we performed a yeast two-hybrid screen[6] using *Xenopus* Smad1. This yielded a protein that interacts with Smad1 and has significant homology to the Hect subclass of E3 ubiquitin ligases[7], which selectively target proteins for ubiquitination and degradation by the 26S proteasome[8]. We named this gene and a closely related human homologue, *XSmurf1* and *hSmurf1*, respectively (for *Xenopus* and human SMAD ubiquitination regulatory factor-1). Both encoded proteins comprise 731 amino acids, share 91%

sequence identity and are most closely related to Pub1, a ubiquitin ligase in *Schizosaccharomyces pombe* that regulates mitosis by targeting Cdc25 for proteasomal degradation[9]. Other members of this class of E3 ubiquitin ligases[7] include Nedd4 and yeast Rsp5[10,11]. Smurf1 shares distinctive structural features with these E3 ubiquitin ligases (Fig. 1a). These include an amino-terminal phospholipid/ calcium-binding C2 domain[12,13], two WW domains[14], which facilitate protein–protein interactions by binding to PPXY motifs on partner proteins, and a carboxy-terminal HECT domain[7], which catalyses ubiquitin ligation onto target proteins.

In *Xenopus* embryonic development, *XSmurf1* mRNA was expressed from the egg stage to the swimming tadpole, with maximum levels observed in the stages from egg to gastrula (Fig. 1b). The bulk of *XSmurf1* mRNA in early development represents maternal transcripts accumulated during oogenesis. Whole-mount *in situ* hybridization (Fig. 1c) revealed that the maternal *XSmurf1* transcripts were localized to the upper, animal-
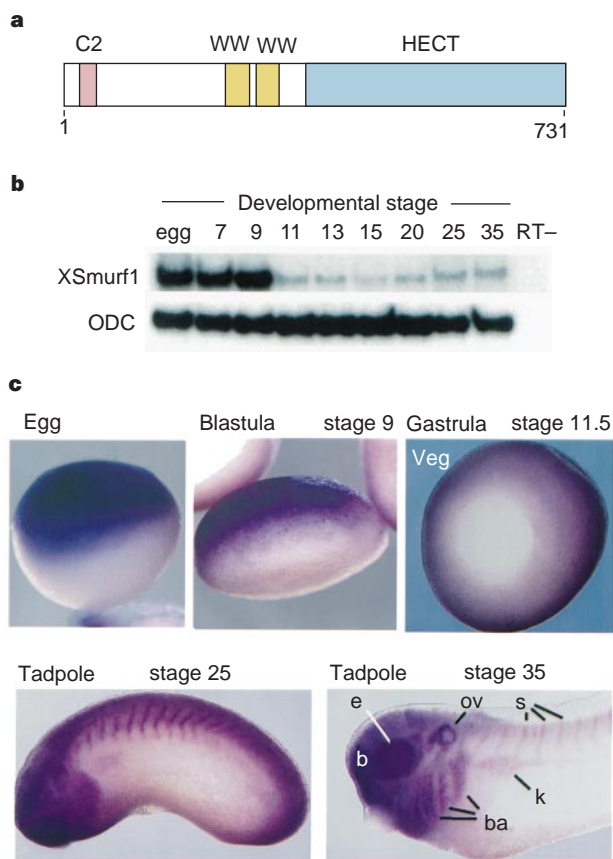

Figure 1 *Smurf1* encodes an E3 ubiquitin ligase expressed in early *Xenopus* development. **a**, Schematic of conserved protein domains found in *Xenopus* and human Smurf1 proteins: a lipid/Ca^{2+}-binding (C2) domain at residues 22–37, WW protein interaction domains at residues 236–271 and 282–311, and a catalytic Hect domain at residues 347–731. See Supplementary Information for a detailed comparison of these proteins. **b**, Expression of XSmurf1 in *Xenopus* embryonic development, assayed by RT-PCR. Embryonic stages[30] correspond to blastula (stages 7 and 9), gastrula (stages 11 and 13), neurula (stages 15 and 20) and tadpole (stages 25 and 35). Ornithine decarboxylase (ODC) expression normalizes RNA recovery and reaction integrity. RT– represents PCR on mock cDNA (no reverse transcriptase). **c**, Whole-mount *in situ* hybridization of XSmurf1 in developing albino *Xenopus* embryos. In the egg and blastula, XSmurf1 transcripts are localized to the animal pole (dark purple stain). Gastrula view is from the vegetal pole (Veg); yolk plug not stained. Lower panels, lateral views of stage 25 and 35 tadpoles; brain (b), eye (e), otic vesicle (ov), somites (s), branchial arches (ba) and kidney (k).
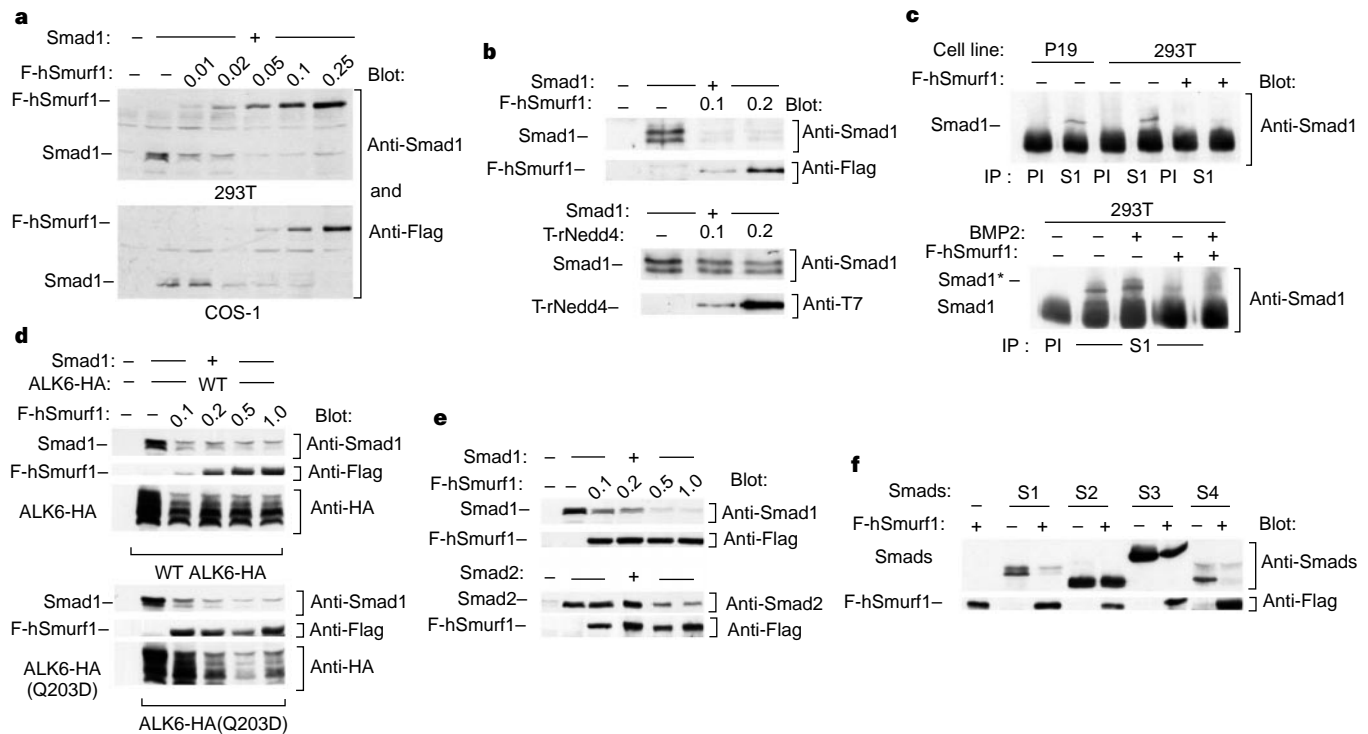
pole half of the egg and cleavage-stage blastula, which was confirmed by northern blot analysis on total animal and vegetal RNA from the blastula (data not shown). At gastrulation, *XSmurf1* mRNA was distributed uniformly in embryonic ectoderm and involuting mesoderm, but expression gradually localized to the nervous system (data not shown). At early tadpole stages, XSmurf1 was expressed in the central nervous system, eye, branchial arches, kidney and somites (Fig. 1c). This embryonic expression pattern of XSmurf1 coincides partly with the expression patterns of genes encoding Smad1 and BMP at similar stages[15–18].

Smurf1 contains a putative E3 ligase, or Hect domain, and is a candidate protein that interacts with Smad1. We therefore investigated whether Smurf1 regulates steady-state levels of Smad1 protein. In two mammalian cell lines, 293T and COS-1, co-expression of Smad1 with hSmurf1 produced a significant, dose-dependent decrease in steady-state levels of Smad1 protein. This was specific for hSmurf1, as overexpression of Nedd4, a related E3 ubiquitin ligase, had only a slight effect on Smad1 protein (Fig. 2b). Transient hSmurf1 expression also strongly reduced the amount of endogenous Smad1 in 293T cells (Fig. 2c), both in the absence and presence of BMP stimulation. Furthermore, co-expressing Smad1 together with the activated BMP type-I receptor ALK6 (also known as BMPRIB) did not alter hSmurf1-dependent decreases in Smad1 levels (Fig. 2d). In the course of these latter experiments, we often observed decreased steady-state levels of the activated receptor in the presence of hSmurf1. This effect was not observed for activated TGF-β receptors (data not shown) and may be due to Smad1 recruiting some hSmurf1 to the activated receptor, with subsequent enhancement of receptor turnover. Together, these results show that expression of hSmurf1 causes dose-dependent decreases in Smad1 steady-state levels that occur independently of activation of Smad1 by the type-I BMP receptor.

To determine whether Smurf1 effects were exclusive to Smad1, we studied Smad2, a receptor-regulated SMAD that functions in TGF-β- and activin-signalling pathways. Relative to Smad1, hSmurf1 had a smaller effect on steady-state levels of Smad2 protein, which occurred only at the highest levels of hSmurf1 expression (Fig. 2e). Similarly, hSmurf1 had little or no effect on Smad3 or Smad4, but elicited a strong decrease in Smad5 protein, which is closely related to Smad1 (Fig. 2f). Thus, hSmurf1 regulates the steady-state levels of Smad1 and Smad5, two receptor-regulated SMADs that function in BMP signalling.

To investigate whether hSmurf1 regulates SMAD degradation, we analysed Smad1 turnover by pulse-chase experiments. In the absence of hSmurf1, Smad1 had a half-life of approximately 6 h. However, in the presence of hSmurf1, Smad1 turnover was enhanced, and displayed a half-life of less than 2 h (Fig. 3a). To determine whether decreases in Smad1 protein were dependent on the proteasome, we tested two inhibitors. In COS-1 cells, LLnL treatment prevented hSmurf1-dependent decreases in Smad1 (Fig. 3b). We were unable to assess LLnL in 293T cells owing to toxic effects, but the inhibitor lactacystin[19] also suppressed hSmurf1-dependent loss of Smad1 protein in 293T cells (Fig. 3b). These data demonstrate that hSmurf1 induces Smad1 degradation through the proteasome.

We next tested whether hSmurf1 enhances Smad1 turnover through ubiquitination. We transfected 293T cells with HA-tagged ubiquitin[20] together with Flag-tagged Smad1, in the presence or absence of Myc-tagged hSmurf1. In the absence of hSmurf1, Smad1 displayed little or no detectable ubiquitination; however, upon co-transfection with hSmurf1 we observed the appearance of a ladder of ubiquitin-conjugated Smad1 products (Fig. 3c). To confirm that ubiquitination of Smad1 required the catalytic activity of the Hect domain in hSmurf1, we constructed a point mutant of hSmurf1 (hSmurf1(C710A)) that targets the cysteine residue that is thought to form a thiolester bond with ubiquitin[7]. In contrast to wild-type hSmurf1, expression of hSmurf1 (C710A) did not yield

Figure 2 Smurf1 expression decreases the steady-state level of Smad1 and Smad5. COS-1 (**a**) or 293T (**a–f**) cells were transiently transfected with the indicated mammalian expression constructs. In **a**, **b**, **d** and **e**, the amount of Flag-tagged hSmurf1 (F–hSmurf1) DNA is shown in micrograms. Steady-state protein levels were determined by immunoblotting aliquots of total cell lysates using the appropriate antibodies as shown. **a**, **b**, hSmurf1, but not Nedd4, decreases Smad1 steady-state levels. Smad1 protein levels were determined in cells transfected with Smad1 and increasing concentrations of Flag-tagged hSmurf1 (**a**) or T7-tagged rat Nedd4 (T–rNedd4)[13](**b**). **c**, hSmurf1 decreases endogenous Smad1 levels. Lysates prepared from P19, 293T (–) or 293T cells transiently expressing Flag-tagged hSmurf1 (+) were subjected to immunoprecipitation (IP) with preimmune (PI) or anti-Smad1 (S1) antibodies, followed by anti-Smad1

immunoblotting. Bottom panel: 293T cells were incubated in the presence (+) or absence (–) of BMP2 for 30 min before analysis of Smad1 levels. The migration of phosphorylated Smad1 is indicated (Smad1*). F–hSmurf1 expression was confirmed by immunoblotting total cell lysates (not shown). **d**, hSmurf1 reduces Smad1 steady-state levels independent of receptor activation. Smad1 levels were assessed in cells co-expressing Smad1, F–hSmurf1 and wild-type (WT) or activated (Q203D) ALK6/BMPRIB-HA receptors (anti-HA). **e**, **f**, hSmurf1 preferentially targets Smad1 and Smad5. Steady-state levels of transfected Smad1 or Smad2 protein were examined in lysates from cells expressing increasing amounts of F–hSmurf1 (**e**). The steady-state level of transfected Smad1, Smad3, Smad4 or Smad5 in the presence (+) or absence (–) of F–hSmurf1 was assessed by immunoblotting cell lysates with the appropriate antibody (anti-Smads).

ubiquitinated Smad1 (Fig. 3d) and, moreover, hSmurf1 (C710A) did not induce decreased steady-state levels of Smad1 protein compared with wild-type hSmurf1 (Fig. 3e). Thus, hSmurf1 controls Smad1 steady-state levels by inducing poly-ubiquitination of Smad1 through its Hect domain, with subsequent degradation through the proteasome.

To assess how Smurf1 selectively targets Smad1 and Smad5 for degradation, we investigated the interaction of Smurf1 with SMAD proteins. Assays performed *in vitro* showed that XSmurf1 selectively bound to Smad1, but not to Smad2 and Smad4 (Fig. 4a). In mammalian cells, we were unable to detect interactions between wild-type hSmurf1 and Smad1. However, the interaction between the Smurf1 ubiquitin ligase and its Smad1 substrate may be transient in intact cells. Therefore we examined the ubiquitin-ligase mutant of hSmurf1 and found that hSmurf1(C710A) formed a stable complex with Smad1 and Smad5, but associated only weakly with Smad2 (Fig. 4b). Furthermore, this interaction was unaffected by co-expression of the constitutively active BMP type-I receptor, ALK2 (ref. 21, and data not shown), which is consistent with the notion that hSmurf1 regulates Smad1 turnover independent of BMP signalling. The linker regions of receptor-regulated SMADs contain a PPXY sequence, which is a conserved motif recognized by WW domains[14], such as those found in both XSmurf1 and hSmurf1. Consequently, we tested whether hSmurf1 would interact with Smad1 in which the PY motif was deleted (residues 223–227,

inclusive). Unlike wild-type Smad1, there was little if any association between Smad1(ΔPY) and hSmurf1(C710A) (Fig. 4c), and Smad1(ΔPY) was resistant to hSmurf1-mediated degradation (Fig. 4d). It therefore seems that Smurf1 associates specifically with Smad1 and Smad5 through interactions between the PY motif in Smad1 and the WW domains of Smurf1.

In cultured cells, hSmurf1 downregulates the amount of BMP-pathway-specific Smad1 and Smad5 proteins. We therefore tested whether XSmurf1 might regulate BMP signalling in the ectodermal and mesodermal embryonic germ layers of the *Xenopus* embryo. In mesoderm of the ventral marginal zone (VMZ), BMP signals specify tissues such as blood and mesenchyme. However, if BMP signals are blocked in the VMZ, dorsal mesodermal tissues such as muscle develop in a process referred to as dorsalization[3]. Expression of ectopic XSmurf1 in the VMZ triggered formation of ectopic axial structures in the ventral side of resulting tadpoles (Fig 5a), which is characteristic of dorsalization resulting from BMP inhibition. This correlated with inhibition of expression of markers for blood differentiation, and was concomitant with activation of muscle-differentiation markers in treated VMZ explants (Fig 5a, right panel). In both intact tadpoles and VMZ explants, co-expression of ectopic Smad1 together with XSmurf1 reversed the dorsalizing effects of XSmurf1, demonstrating specificity for the BMP pathway. Furthermore, overexpression of XSmurf1 in cells of the dorsal marginal zone (DMZ), which forms head and axial mesodermal

tissues, had no effect (data not shown). Smad2 mediates activin/nodal/Vg1 signals during development of the *Xenopus* dorsal axis[3,5,22]. Therefore this latter observation is consistent with our findings in cultured cells that hSmurf1 does not target Smad2 to any appreciable extent.

In the ectodermal germ layer of *Xenopus* embryos, endogenous BMP signals specify epidermis, but if BMP signals are reduced or eliminated, the ectoderm differentiates into cement gland or neural tissue, respectively[23]. Furthermore, varying Smad1 or Smad5 levels in *Xenopus* ectoderm also alters cell fate[18,24,25]. Thus, the localization of *XSmurf1* mRNA in the *Xenopus* animal pole indicates that XSmurf1 may regulate ectodermal differentiation and pattern by modulating BMP signalling. We therefore overexpressed XSmurf1 in animal pole tissue (animal caps) and found that XSmurf1 triggered neural and cement-gland differentiation, which is characteristic of inhibited BMP signalling. These effects were reversed by co-expressing Smad1 (Fig. 5b). We suggest that a normal embryonic function of XSmurf1 is to provide an intracellular, cell-autonomous mechanism for antagonizing BMP signalling through alterations in levels of Smad1 or Smad5 protein. This regulation might complement the function of BMP inhibitors secreted by the Spemann organizer, such as noggin, chordin and follistatin, which bind and block BMP ligands.

To test whether XSmurf1 specifically inhibits the biological effects of BMP signals at the SMAD level, we co-expressed XSmurf1 in

combination with Smad1 or Smad2 in *Xenopus* animal caps. Overexpression of particular receptor-regulated SMADs in animal caps mimics the effects of their corresponding TGF-β ligands or activated receptors. Thus, injection of *Smad1* mRNA induces ventral/posterior mesoderm, like BMP ligands, whereas injection of *Smad2* mRNA induces dorsal (Spemann organizer) mesoderm, like activin, Vg1 and nodal ligands. Injection of *Smad1* mRNA alone (1 ng) in animal caps induced the ventral/posterior mesoderm-specific genes *Xhox3* and *Xcad1*. However, co-injection of *XSmurf1* mRNA blocked Smad1-dependent induction of these genes at all *XSmurf1* doses tested (Fig. 6a), demonstrating that XSmurf1 antagonizes Smad1. We next tested XSmurf1 effects on Smad2 activity by injecting animal caps with a limiting dose of *Smad2* mRNA (50 pg) that was sufficient to induce muscle-specific *myoD*, a marker of dorsal/lateral mesoderm, but insufficient to induce *goosecoid*, a marker gene specific to the Spemann organizer (Fig. 6b,c). Co-expression of any dose of *XSmurf1* (up to 400 pg mRNA) did not interfere with Smad2-dependent induction of the *myoD* gene (Fig. 6b), which is consistent with our data showing that human or *Xenopus* Smurf1 does not efficiently target Smad2. When we monitored *goosecoid*, we observed that, as the dose of *XSmurf1* mRNA was increased from 50 to 400 pg, *goosecoid* gene expression was triggered (Fig. 6b). This mimicked the effects of injecting high doses of *Smad2* alone. Injection of 50 pg *Smad2* and 100 pg *XSmurf1* mRNA triggered *goosecoid* expression to almost the same degree as a
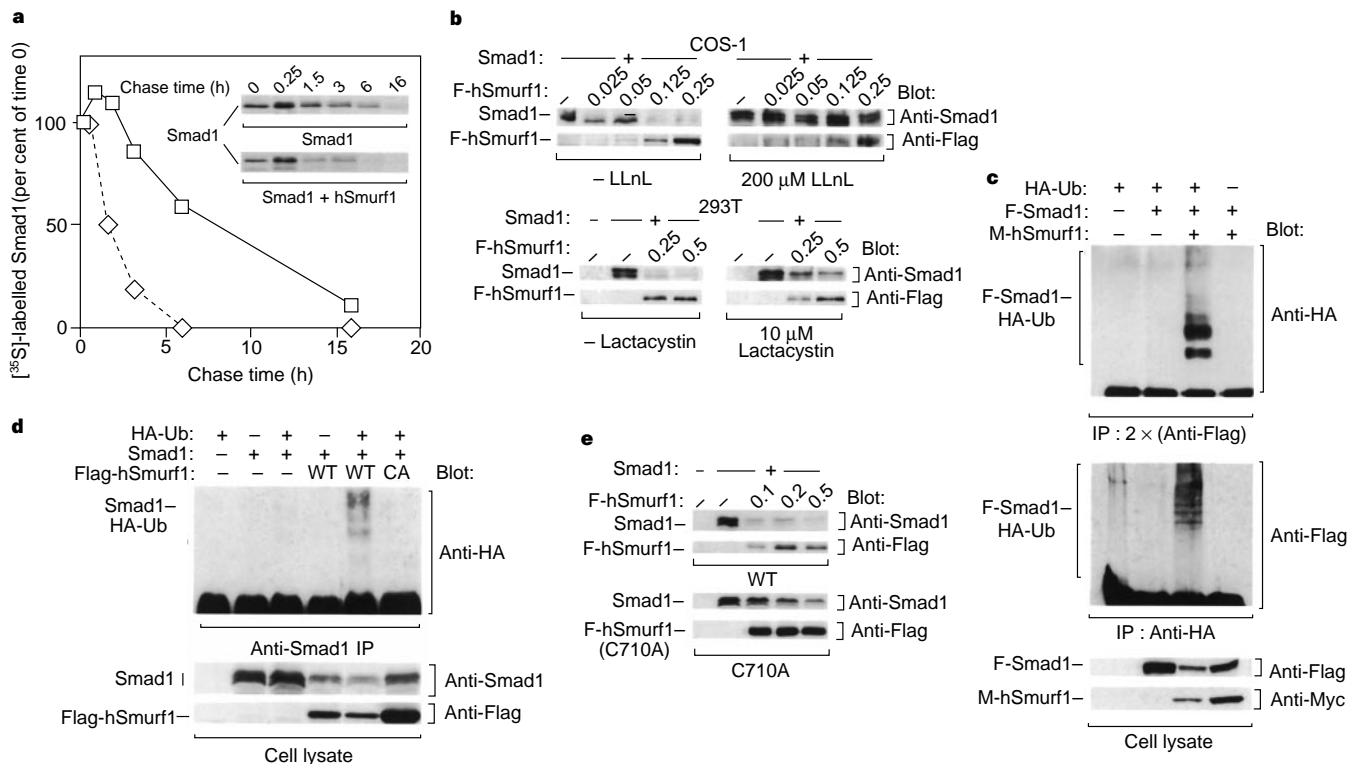

Figure 3 hSmurf1 induces Smad1 turnover and ubiquitination. **a**, COS-1 cells transfected with Smad1 and Flag-tagged hSmurf1 (F–hSmurf1) were pulse-labelled with ^{35}S-methionine and then chased for the indicated times in media containing unlabelled methionine. ^{35}S-labelled Smad1 in anti-Smad1 immuno-precipitates (inset) was quantified by phosphorimaging and the levels in control cells (squares) and hSmurf1-expressing cells (diamonds) are plotted relative to the amount present at time 0. **b**, Effect of proteasome inhibitors on Smad1 stability. The indicated cells, transfected with Smad1 and increasing amounts of F–hSmurf1, were treated overnight with or without 200 μM LLnL (top panel) or 10 μM lactacystin (bottom panel), before analysis of Smad1 steady-state levels. **c**, Ubiquitination of Smad1 in 293T cells. Lysates from cells transfected with HA-tagged ubiquitin (HA–Ub), Flag-tagged Smad1 (F–Smad1) and/or Myc-

tagged hSmurf1 (M–hSmurf1) were subjected to immunoprecipitation followed by immunoblotting as indicated. Ubiquitinated species of Smad1 are indicated (F–Smad1-HA-Ub). **d**, **e**, Ubiquitination and loss of Smad1 requires activity of the Smurf1 Hect domain. Lysates from cells transiently expressing HA-ubiquitin, Smad1 and either wild-type (WT) or the C710A mutant of F–hSmurf1 (CA) were subjected to anti-Smad1 immunoprecipitation (anti-Smad1 IP) followed by anti-HA immunoblotting (anti-HA blot) (**d**). Smad1 protein levels (anti-Smad1) were assessed in total cell lysates from 293T cells transfected with Smad1 and increasing amounts of wild-type (WT) or F–hSmurf1(C710A) (**e**). In **b**–**e**, protein expression was confirmed by immunoblotting aliquots of total cell lysates (bottom panels).

fivefold higher (250 pg) dose of *Smad2* alone (Fig. 6c). The induction of *goosecoid* in the presence of *XSmurf1* was *Smad2*-dependent, as *XSmurf1* alone did not activate *goosecoid* at any dose tested. Thus, XSmurf1 enhanced the sensitivity of animal-cap cells to Smad2. Together, these data show that Smurf1 alters the competence of animal-pole cells to respond to different TGF-β signalling pathways by simultaneously inhibiting BMP signals and enhancing activin-like signals. Because receptor-regulated SMADs in the BMP and activin pathways may compete for the common SMAD, Smad4 in *Xenopus* embryos[26,27], Smurf1 may sensitize animal pole cells to Smad2/activin by reducing endogenous Smad1 or Smad5, thus liberating Smad4 and promoting formation of Smad2–Smad4 complexes.

In conclusion, we have shown that TGF-β signalling can be controlled by selective ubiquitination of SMAD signalling molecules. These findings have important implications for the regulation of cell fate in development and, more generally, cell responses to TGF-β signals in diverse biological contexts. The identification of Smurf1, a SMAD-specific E3 ubiquitin ligase, provides the first link between TGF-β signalling and the ubiquitination system. Smurf1 blocks intracellular BMP signals by specifically targeting Smad1 and Smad5 for ubiquitination and proteasomal degradation, independent of BMP receptor activation. This indicates that Smurf1 does not function downstream of activated SMADs to turn off BMP signals but rather controls cell competence to respond to BMPs. In particular, we demonstrate that Smurf1 reduces Smad1 and Smad5 protein levels in cultured cells and affects embryonic patterning by BMP signals in the ectoderm and mesoderm of *Xenopus* embryos. Moreover, changes in the levels of Smurf1 can alter the competence of embryonic cells to respond to different TGF-β signalling pathways, as increased amounts of Smurf1 not only inhibit cellular responses to the Smad1/5 (BMP) pathway, but also simultaneously enhance sensitivity to the Smad2 (activin/TGF-β) pathway. The selective nature of Smurf1-mediated SMAD
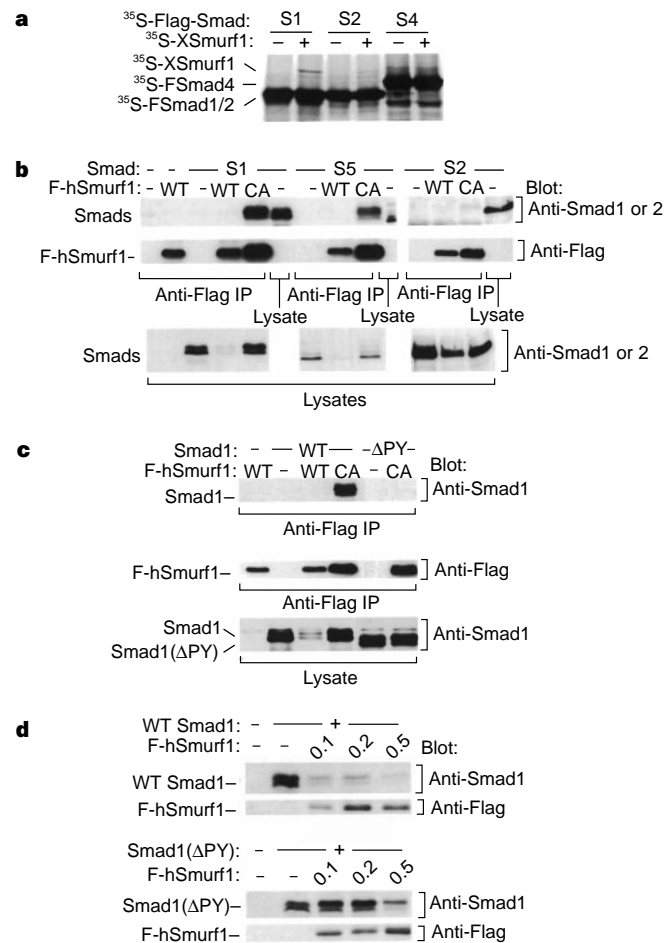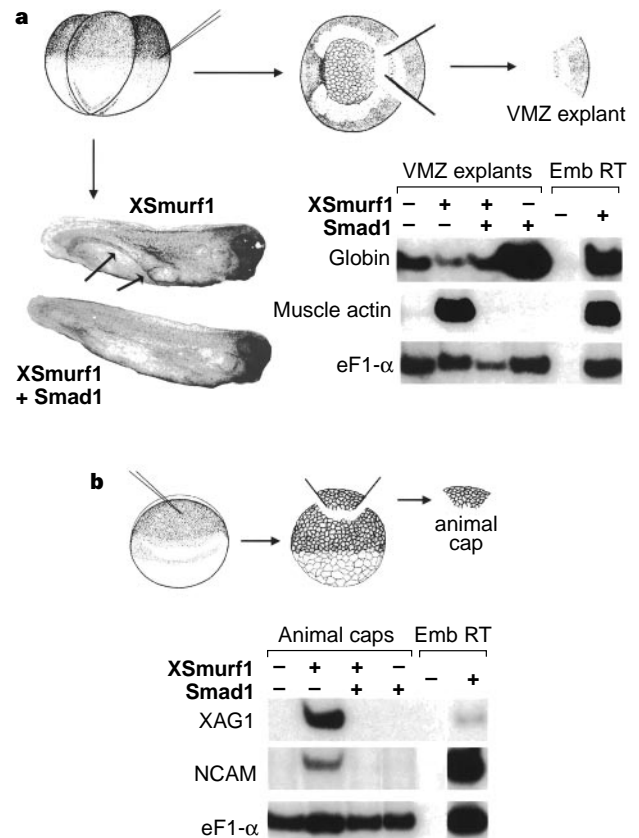

Figure 4 Interaction of Smurf1 and Smads. **a**, XSmurf1 interacts with Smad1 *in vitro*. Interaction between XSmurf1 and Smad1 was assessed by incubating *in vitro*-translated, [35S]Met-labelled XSmurf1 with *in vitro*-translated, [35S]Met-labelled Flag-tagged Smad1, Smad2 or Smad4 immobilized on anti-Flag affinity-gel matrices. **b**, hSmurf1 interacts selectively with Smad1 and Smad5 in mammalian cells. 293T cells transfected with Smad1 (S1), Smad5 (S5) or Smad2 (S2) and either wild-type (WT) or the ubiquitin-ligase mutant C710A (CA) of Flag-tagged hSmurf1 (F–hSmurf1) were subjected to anti-Flag immunoprecipitation followed by immunoblotting with anti-Smad1/5 or anti-Smad2 polyclonal antibody, as appropriate. The levels of F–hSmurf1 in the immunoprecipitates and Smad levels in total cell lysates are shown as indicated. **c**, **d**, The PY motif in Smad1 is an important determinant for interaction with Smurf1. Lysates from 293T cells transfected with Smad1, Smad1(ΔPY) and either wild-type (WT) or mutant (CA) F–hSmurf1 were subjected to anti-Flag immunoprecipitation followed by immunoblotting with anti-Smad1 antibodies to detect associated Smad1 (**c**). Steady-state levels of transfected Smad1 or Smad1(ΔPY) were assessed by immunoblotting total cell lysates from 293T cells expressing increasing amounts of F–hSmurf1.

Figure 5 Smurf1 dorsalizes ventral mesoderm and neuralizes ectoderm of *Xenopus* embryos. **a**, Two ventral blastomeres of four-cell *Xenopus* embryos were injected in the marginal zone with *XSmurf1* mRNA (50 pg per cell), with (+) or without (–) 100 pg *Smad1*. Left, tadpoles developed from injected embryos formed ectopic, dorsal axial structures (arrows). Right, in a parallel experiment, ventral marginal zone (VMZ) explants were excised at early gastrulation and scored by RT-PCR at tadpole stage 28 for expression of the indicated marker genes. **b**, Animal poles of fertilized eggs were injected with 100 pg of *XSmurf1*, with (+) or without (–) *Smad1* mRNA, or were uninjected. Animal-cap explants were analysed by RT-PCR at gastrula stage 11 for expression of XAG, a cement gland marker, and NCAM, a general neural marker. In both **a** and **b**, the two lanes on the far right are control reactions on total embryonic RNA, with (+) or without (–) reverse transcription.
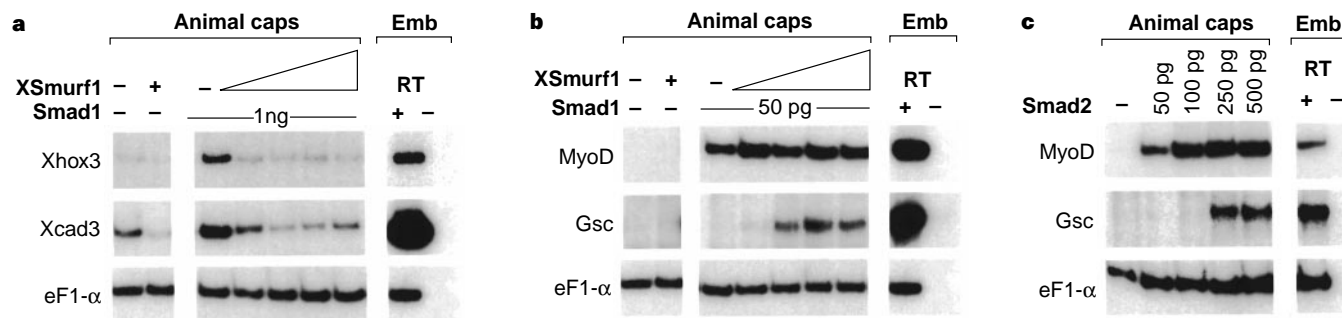
Figure 6 Smurf1 alters embryonic cell competence to respond to Smad1 and Smad2. **a**, XSmurf1 blocks ventral mesoderm induction by Smad1. Animal poles from fertilized eggs were injected with 1 ng *Smad1* mRNA alone, or together with increasing amounts of *XSmurf1* mRNA (gradient), or were not injected. Animal caps were excised from mid-blastula-stage embryos, cultured to late gastrula stage, then scored for *Xhox3* and *Xcad3* expression by RT-PCR. In lanes from left to right, injected doses of *XSmurf1* mRNA were 0, 100, 0, 50, 100, 200 and 400 pg, respectively. **b**, XSmurf1 enhances dorsal mesoderm induction by Smad2. Animal poles from fertilized eggs were injected with a constant amount (50 pg) of *Smad2* mRNA either alone, or together with increasing amounts of *XSmurf1* mRNA (as in **a**), cultured as above, then scored for *goosecoid* and *myoD* expression by RT-PCR. Note that goosecoid expression was triggered from undetectable levels as the dose of *XSmurf1* was increased. **c**, Dose–response of animal caps to Smad2. Amounts of injected *Smad2* mRNA and RT-PCR analysis were as in **b**. Controls in all panels were as in Fig. 5.

ubiquitination and the distinct effects of Smurf1 on cell responses to TGF-β-like factors provides a new mechanism for regulating cell growth, embryonic development, tissue stasis and other processes controlled by SMAD signalling pathways. □

Methods

Cloning of *Smurf1* genes and construction of complementary DNA. A *Xenopus Smad1* cDNA[18] was cloned into the pGBT9 vector and used to screen a *Xenopus* oocyte cDNA library (Clonetech) by the yeast two-hybrid method[6]. A partial cDNA we isolated was used to screen a *Xenopus* stage 9 (blastula) cDNA library to obtain a full-length *XSmurf1* cDNA clone (GenBank accession number AF169310). A human *Smurf1* cDNA encoding all but the first eight amino acids was identified in the expressed-sequence-tag database (AA292123), and full-length hSmurf1 was reconstituted using a fragment of *XSmurf1* cDNA encoding the first eight amino acids. *hSmurf* cDNA was Flag-tagged at its N terminus. The polymerase chain reaction (PCR) was used to generate a ubiquitin-ligase mutant of hSmurf1 in which cysteine 710 was replaced with alanine and the ΔPY mutant of Smad1 in which the PPPAY sequence between amino-acid residues 223–227 was deleted.

Immunoprecipitations and immunoblotting. For immunoprecipitation assays, *Xenopus* Smad1 (ref. 18), mouse Smad4 and human Smad2 (ref. 28) were Flag-tagged at their N termini and translated *in vitro* (rabbit reticulocyte extracts; Promega) in the presence of [^{35}S]-methionine. The Flag-tagged SMADs were bound to anti-Flag antibody-conjugated beads (Kodak), washed in co-immunoprecipitation buffer (10 mM Tris, pH 7.5, 90 mM NaCl, 1 mM EDTA, 1% Triton-X 100, 10% glycerol, 1 mM phenylmethylsulphonylflouride) then incubated with [^{35}S]Met-labelled hSmurf1 in the same buffer. After washing in co- immunoprecipitation buffer, proteins were eluted in gel-loading buffer, separated by SDS–polyacrylamide gel electrophoresis (PAGE) and visualized by autoradiography.

For studies in mammalian cells, COS-1 and 293T cells were transiently transfected using lipofectAMINE (Gibco/BRL) or calcium phosphate precipitation, respectively. Immunoprecipitations and immunoblotting were done using anti-HA (12CA5, Boehringer), anti-Myc (9E10), anti-Flag M2 (Sigma) or anti-T7 (Novagen) monoclonal antibodies, or anti-Smad1/5 or anti-Smad2/3 polyclonal antibodies, as described previously[21]. Detection was achieved using the appropriate horseradish peroxidase (HRP)-conjugated goat anti-mouse or goat anti-rabbit secondary antibodies and enhanced chemiluminescence (Amersham). In experiments that used proteasome inhibitors, transfected COS1 or 293T cells were incubated overnight with 200 μM LLnL or 10 μM lactacystin, respectively, as described previously[29], before analysis of Smad1 protein levels.

Embryo methods and RT-PCR. All *Xenopus* embryo methods and PCR coupled with reverse transcription (RT-PCR) were done as described[18]. Primers for RT-PCR on *XSmurf1* were 5′-GTCCTGTGACTGGAACCC-3′ (sense) and 5′-GAGGACTGCTAGACAAT-3′ (antisense), with 5′ ends respectively located at positions 482 and 726 in the cDNA. Other primers used are described on the *Xenopus* Molecular Marker Homepage (http://vize222.zo.utexas.edu).

Pulse-chase analysis. COS-1 cells were transfected as indicated, and two days post-transfection the cells were labelled for 10 min at 37 °C with 50 μCi ^{35}S-methionine per ml in methionine-free Dulbecco's modified Eagle's medium (DMEM; Pulse). Cell layers were then washed two times and incubated in DMEM + 10% fetal calf serum (FCS) for the indicated time periods (Chase). At each time point of the chase, cell lysates were immunoprecipitated with an anti-Smad1 polyclonal antibody, resolved by SDS–PAGE and visualized by autoradiography. A Phosphorimager (Molecular Dynamics) was used to quantify metabolically labelled Smad1 present at each time point.

Ubiquitination assay. 293T cells were transfected with HA-tagged ubiquitin, Flag-tagged or untagged Smad1, and either Flag-tagged or Myc-tagged hSmurf1 or Flag–hSmurf1 (C710A) as indicated. Two days post-transfection, cell lysates were subjected to either anti-Flag or anti-HA immunoprecipitation. Anti-Flag immunoprecipitates were boiled in 1% SDS for 5 min, diluted with TNTE (50 mM Tris-HCl, pH 7.4, 150 mM NaCl, 1 mM EDTA, 0.1% TritonX-100) and subjected to a second anti-Flag immunoprecipitation before immunoblotting with anti-HA to detect HA-ubiquitin conjugated to Smad1. Anti-HA immunoprecipitates were immunoblotted with anti-Flag to visualize HA-ubiquitinated Smad1. Expression levels of transiently expressed Smad1 and hSmurf1 were analysed by immunoblotting aliquots of total cell lysates with the appropriate antibodies.

1. Kingsley, D. M. The TGF-β superfamily: new members, new receptors, and new genetic tests of function in different organisms. *Genes Dev.* **8,** 133–146 (1994).
2. Moses, H. L. & Serra, R. Regulation of differentiation by TGF-beta. *Curr. Opin. Genet. Dev.* **6,** 581–586 (1996).
3. Harland, R. & Gerhart, J. Formation and Function of Spemann's organizer. *Annu. Rev. Cell Biol.* **13,** 611–667 (1997).
4. Massague, J. TGF-beta signal transduction. *Annu. Rev. Biochem.* **67,** 753–791 (1998).
5. Whitman, M. Smads and early developmental signaling by the TGFβ superfamily. *Genes Dev.* **12,** 2445–2462 (1998).
6. Bartel, P. & Fields, S. Analyzing protein-protein interactions using two-hybrid system. *Methods Enzymol.* **254,** 241–263 (1995).
7. Huibregtse, J. M., Scheffner, M., Beaudenon, S. & Howley, P. M. A family of proteins structurally and functionally related to the E6-AP ubiquitin-protein ligase. *Proc. Natl Acad. Sci. USA* **92,** 2563–2567 (1995). [Published erratum appears in *Proc. Natl Acad. Sci. USA* **92,** 5249 (1995).]
8. Hershko, A. & Ciechanover, A. The ubiquitin system. *Annu. Rev. Biochem.* **67,** 425–479 (1998).
9. Nefsky, B. & Beach, D. Pub1 acts as an E6-AP-like protein ubiquitin ligase in the degradation of cdc25. *EMBO J.* **15,** 1301–1312 (1996).
10. Scheffner, M., Huibregtse, J. M., Vierstra, R. D. & Howley, P. M. The HPV-16 E6 and E6-AP complex functions as a ubiquitin-protein ligase in the ubiquitination of p53. *Cell* **75,** 495–505 (1993).
11. Hein, C., Springael, J., Volland, C., Haguenauer-Tsapis, R. & Andre, B. NPl1, an essential yeast gene involved in induced degradation of Gap1 and Fur4 permeases, encodes the Rsp5 ubiquitin-protein ligase. *Mol. Microbiol.* **18,** 77–87 (1995).
12. Nalefski, E. A. & Falke, J. J. The C2 domain calcium-binding motif: structural and functional diversity. *Protein Sci.* **5,** 2375–2390 (1996).
13. Plant, P. J., Yeger, H., Staub, O., Howard, P. & Rotin, D. The C2 domain of the ubiquitin protein ligase Nedd4 mediates Ca^{2+}-dependent plasma membrane localization. *J. Biol. Chem.* **272,** 32329–32336 (1997).

14. Rotin, D. WW (WWP) domains: from structure to function. *Curr. Top. Microbiol. Immunol.* **228**, 115–133 (1998).
15. Fainsod, A., Steinbeisser, H. & De Robertis, E. M. On the function of BMP-4 in patterning the marginal zone of the *Xenopus* embryo. *EMBO J.* **13**, 5015–5025 (1994).
16. Hemmati-Brivanlou, A. & Thomsen, G. H. Ventral mesodermal patterning in *Xenopus* embryos: expression patterns and activities of BMP-2 and BMP-4. *Dev. Genet.* **17**, 78–89 (1995).
17. Nishimatsu, S. & Thomsen, G. H. Ventral mesoderm induction and patterning by BMP heterodimers in *Xenopus* embryos. *Mech. Dev.* **74**, 75–88 (1997).
18. Thomsen, G. H. *Xenopus* mothers against decapentaplegic is an embryonic ventralizing agent that acts downstream of the BMP-2/4 receptor. *Development* **122**, 2359–2366 (1996).
19. Fenteany, G. *et al.* Inhibition of proteasome activities and subunit-specific amino-terminal threonine modification by lactacystin. *Science* **268**, 726–731 (1995).
20. Treier, M., Staszewski, L. M. & Bohmann, D. Ubiquitin-dependent c-Jun degradation in vivo is mediated by the delta domain. *Cell* **78**, 787–798 (1994).
21. Macias-Silva, M., Hoodless, P. A., Tang, S. J., Buchwald, M. & Wrana, J. L. Specific activation of Smad1 signaling pathways by the BMP7 type I receptor, ALK2. *J. Biol. Chem.* **273**, 25628–25636 (1998).
22. Hoodless, P. A. *et al.* Dominant-negative Smad2 mutants inhibit activin/Vg1 signaling and disrupt axis formation in *Xenopus. Dev. Biol.* **207**, 364–379 (1999).
23. Hemmati-Brivanlou, A. & Melton, D. Vertebrate embryonic cells will become nerve cells unless told otherwise. *Cell* **88**, 13–17 (1997).
24. Wilson, P. A., Lagna, G., Suzuki, A. & Hemmati-Brivanlou, A. Concentration-dependent patterning of the *Xenopus* ectoderm by BMP4 and its signal transducer Smad1. *Development* **124**, 3177–3184 (1997).
25. Suzuki, A., Chang, C., Yingling, J. M., Wang, X. F. & Hemmati-Brivanlou, A. Smad5 induces ventral fates in *Xenopus* embryos. *Dev. Biol.* **184**, 402–405 (1997).
26. Lagna, G., Hata, A., Hemmati-Brivanlou, A. & Massague, J. Partnership between DPC4 and SMAD proteins in TGF-β signalling pathways. *Nature* **383**, 832–836 (1996).
27. Candia, A. F. *et al.* Cellular interpretation of multiple TGF-beta signals: intracellular antagonism between activin/BVg1 and BMP-2/4 signaling mediated by Smads. *Development* **124**, 4467–4480 (1997).
28. Eppert, K. *et al.* MADR2 maps to 18q21 and encodes a TGFβ regulated MAD-related protein that is functionally mutated in colorectal carcinoma. *Cell* **86**, 543–552 (1996).
29. Ward, C. L., Omura, S. & Kopito, R. R. Degradation of CFTR by the ubiquitin-proteasome pathway. *Cell* **83**, 121–127 (1995).
30. Nieuwkoop, P. D. & Faber, J. *Normal Table of* Xenopus laevis *(Daudin)* (North Holland, Amsterdam, 1967).

Trigger factor and DnaK cooperate in folding of newly synthesized proteins

Elke Deuerling, Agnes Schulze-Specking, Toshifumi Tomoyasu, Axel Mogk & Bernd Bukau

Institut für Biochemie und Molekularbiologie, Hermann-Herder-Strasse 7, 79104 D-Freiburg, Germany

The role of molecular chaperones in assisting the folding of newly synthesized proteins in the cytosol is poorly understood. In *Escherichia coli*, GroEL assists folding of only a minority of proteins[1] and the Hsp70 homologue DnaK is not essential for protein folding or cell viability at intermediate growth temperatures[2]. The major protein associated with nascent polypeptides is ribosome-bound trigger factor[3,4], which displays chaperone and prolyl isomerase activities *in vitro*[3,5,6]. Here we show that Δ*tig::kan* mutants lacking trigger factor have no defects in growth or protein folding. However, combined Δ*tig::kan* and Δ*dnaK* mutations cause synthetic lethality. Depletion of DnaK in the Δ*tig::kan* mutant results in massive aggregation of cytosolic proteins. In Δ*tig::kan* cells, an increased amount of newly synthesized proteins associated transiently with DnaK. These findings show *in vivo* activity for a ribosome-associated chaperone, trigger factor, in general protein folding, and functional cooperation of this protein with a cytosolic Hsp70. Trigger factor and DnaK cooperate to promote proper folding of a variety of *E. coli* proteins, but neither is essential for folding and viability at intermediate growth temperatures.

Because trigger factor can associate with ribosomes and nascent polypeptide chains, it is a prime candidate for a chaperone that is dedicated to assist folding of newly synthesized proteins. To elucidate its *in vivo* role genetically, we replaced the complete coding sequence of the *tig* gene (encoding trigger factor) with a kanamycin cassette (Fig. 1a). The Δ*tig::kan* mutant lacking trigger factor was viable and showed no growth defects between 15 and 42 °C in rich (Fig. 1b) and minimal media (not shown). Furthermore, Δ*tig::kan* mutants showed no defects in protein folding at 30 and 37 °C, as judged by unaltered specific activities of a reporter enzyme (firefly luciferase) and solubility of cellular proteins. Trigger factor is thus not essential for viability and protein folding in *E. coli*.

We investigated whether other chaperones compensate for the missing activity of trigger factor in Δ*tig::kan* cells by determining the phenotypes resulting from combining the Δ*tig::kan* allele with additional chaperone-gene mutations. The Δ*tig::kan* allele could be transduced with normal efficiency into the chromosomes of Δ*htpG::lacZ* (ref. 7), *secB::Tn5* (ref. 8), Δ*ibpAB::kan* (unpublished results) and temperature-sensitive *groEL* mutants (L140, L673 and L44)[9] without apparent alteration of the existing growth phenotypes. However, it could not be introduced into Δ*dnaK52* mutant cells[10], which lack DnaK and have low levels of the DnaJ co-chaperone. This finding was further substantiated by co-transduction experiments in which a Tn*10* selective marker (*zba-3054::Tn10*) placed close to the Δ*tig::kan* allele was transduced into Δ*dnaK52* and *dnaK*⁺ cells. The co-transduction frequency of the Δ*tig::kan* allele was 83% in *dnaK*⁺ cells and 0% in Δ*dnaK52* mutant cells. Combination of the Δ*tig::kan* and Δ*dnaK52* mutations thus causes synthetic lethality.

To investigate the cause of the synthetic lethality, we constructed Δ*tig::kan* and *tig*⁺ strains in which expression of the chromosomal *dnaK dnaJ* operon is under the control of the IPTG-regulatable promoter $P_{A1/lacO-1}$ ($P_{IPTG}dnaKJ$, Fig. 1a)[11]. On plates containing 1 mM IPTG, the $P_{IPTG}dnaKJ$ Δ*tig::kan* and $P_{IPTG}dnaKJ$ *tig*⁺ strains formed colonies at all temperatures tested (15, 30, 37 and 42 °C). On plates lacking IPTG, the $P_{IPTG}dnaKJ$ *tig*⁺ cells did not form colonies at 15 and 42 °C (Fig. 1b), consistent with the cold-sensitive and heat-sensitive phenotype of Δ*dnaK52* mutants[12]. In the absence of IPTG, $P_{IPTG}dnaKJ$ Δ*tig::kan* cells did not form colonies at any temperature tested (Fig. 1b); growth of these mutants at 30 and 37 °C was restored by expression of the *tig* gene from plasmids (not shown). The onset of synthetic lethality could also be monitored in liquid medium (Fig. 1c). After overnight growth in medium with IPTG, $P_{IPTG}dnaKJ$ Δ*tig::kan* and $P_{IPTG}dnaKJ$ *tig*⁺ cells were diluted into medium lacking IPTG. DnaK and DnaJ levels decreased from about twice wild-type levels to undetectable amounts after 8 h growth without IPTG (time point 3, Fig. 1c). $P_{IPTG}dnaKJ$ Δ*tig::kan* cells depleted for DnaK and DnaJ started to show slower growth after 8 h (time point 3). At 8 and 10 h (time points 3 and 4), viability (determined as plating efficiency) decreased by 3 and 5 orders of magnitude, respectively, below the $P_{IPTG}dnaKJ$ Δ*tig::kan* control grown with IPTG.

To account for synthetic lethality, we first ruled out that it resulted from DnaK's regulatory role as a negative modulator of σ³², the transcriptional activator of chaperone and protease genes of the heat-shock regulon[13]. Accordingly, overproduction of chaperones and proteases resulting from DnaK and DnaJ depletion may be poisonous for Δ*tig::kan* cells. We artificially induced the heat-shock response in Δ*tig::kan* cells using a plasmid expressing the *rpoH* gene (encoding σ³²) under the control of an IPTG-inducible promoter[14]. IPTG-induced chaperone overproduction was at least as high as chaperone overproduction caused by DnaK and DnaJ depletion (monitored, for example, for GroEL, Fig. 1d) but did not affect the viability of Δ*tig::kan* cells at 30 and 37 °C (Fig. 1d, lower panel).

To investigate whether synthetic lethality is caused by protein-